MOLECULAR CHEMISORPTION OF O_2 ON OXIDIZED Pd(111)

By

JOSE ANGEL HINOJOSA JR.

A THESIS PRESENTED TO THE GRADUATE SCHOOL
OF THE UNIVERSITY OF FLORIDA IN PARTIAL FULFILLMENT
OF THE REQUIREMENTS FOR THE DEGREE OF
MASTER OF SCIENCE

UNIVERSITY OF FLORIDA

2007

To my wife Beverly, and my family.

ACKNOWLEDGMENTS

I gratefully acknowledge Dr. Helena Hagelin-Weaver, Dr. Aravind Asthagiri, and Dr. Scott Perry for their guidance and interest in my education. I thank my advisor, Dr. Jason Weaver for his patience, support, and words of encouragement. I also thank my research group members who have made my research a fulfilling experience. I also gratefully acknowledge financial support for this work provided by the Department of Energy, Office of Basic Energy Science, Catalysis and Chemical Transformations Division through grant number DE-FG02-03ER15478 and the SEAGEP program.

TABLE OF CONTENTS

LIST OF FIGURES

Abstract of Thesis Presented to the Graduate School
of the University of Florida in Partial Fulfillment of the
Requirements for the Degree of Master of Science

MOLECULAR CHEMISORPTION OF O_2 ON OXIDIZED Pd(111)
By

Jose Angel Hinojosa Jr.

December 2007

Chair: Jason F. Weaver
Major: Chemical Engineering

In this work, we oxidized Pd(111) in ultrahigh vacuum (UHV) using an O atom beam, and investigated the molecular chemisorption of O_2 on the oxidized surface using temperature programmed desorption (TPD). We find that the O_2 molecules chemisorb readily on oxidized Pd(111) at 85 K, reaching a saturation coverage of 0.33 ML on a surface covered with 3 ML (monolayer) of Pd oxide. The O_2 TPD spectrum from the oxidized surface at O_2 saturation exhibits four features centered at 118 K, 227 K, 275 K and 315 K associated with the desorption of chemisorbed O_2 molecules. Comparison with O_2 TPD from clean Pd(111) demonstrates that about half of the O_2 molecules on oxidized Pd(111) are more strongly bound than on the metallic surface. Experiments with co-adsorbed $^{16}O_2$ and $^{18}O_2$ further reveal that O_2 molecules dissociate negligibly on the oxidized surface. We also find that O_2 molecules chemisorb only in small quantities (< 0.03 ML) on the p(2×2) and 2D oxide phases of atomic oxygen on Pd(111), indicating that these phases have much weaker binding affinities toward O_2 than the 3D oxide (PdO) generated in our experiments. Finally, temperature programmed reaction spectra of co-adsorbed $^{18}O_2$ and CO demonstrate that both PdO and molecularly adsorbed O_2 are reactive in CO oxidation, with the molecular O_2 exhibiting slightly higher reactivity. The results of this study may have implications for understanding Pd oxidation catalysis at high pressures given

that we find relatively strong binding states of O_2 on oxidized Pd(111) and observe that these molecules are reactive toward CO.

CHAPTER 1
INTRODUCTION

Literature Review

Late transition metals are critical in industrial applications of oxidation catalysis. Palladium in particular is a highly effective catalyst for the oxidation of carbon monoxide [1-3] in automobile catalytic converters and methane oxidation [4-11] in lean gas turbines. There are two thermodynamically stable states for Pd depending on the environmental conditions. For instance, metallic Pd is predominate at high temperature while the surface is oxidized at low temperature [12]. Prior studies provide evidence that PdO is the more active state in the oxidation of methane [4-6,10]. For example, higher reaction rates are reported at the onset of the formation of PdO [13] as compared to the metal surface. Still other studies identify the metallic Pd surface as the active state [9,14,15]. These contradictory findings demonstrate the need for more detailed studies to advance the basic understanding of catalytic oxidation by Pd.

The oxidation of late transition metal surfaces in ultrahigh vacuum (UHV) has proven to be challenging. Several approaches have been developed to produce high concentrations of atomic oxygen on transition metal surfaces in UHV. The traditional approach of using molecular oxygen provides a useful mechanism in studies that target the low coverage chemisorption range of oxygen on Pd. Coverages above this range could not be achieved on Pd by larger O_2 doses [12]. Stronger oxidatants, such as NO_2 and O_3, proved to be successful in producing coverages up to 2.4 ML on Pt [16] and 2.2 ML on Pd [12]. Another approach, which utilizes a high pressure reaction cell, has the capability of producing high oxygen coverages in excess of 20 ML on a variety of Pd surfaces [17]. Atomic oxygen beams also produce high oxygen coverages on both Pd and Pt [18-21]. With these procedures, further understanding of how oxidation occurs and effects on surface properties can be probed.

The oxidation of the Pd(111) surface has been studied in detail previously [12,13,17,22-26]. Pd(111) oxidation first proceeds by chemisorption of atomic oxygen to produce a p(2×2) structure at a surface coverage of 0.25 ML [12]. At a coverage of 0.40 ML several stable states exist, of which one is the (√67×√67) R12.2° structure [23]. A slight increase in the oxygen coverage causes a transformation into the two dimensional (2D) surface oxide, determined to be Pd_5O_4 [25]. Transformation between 2D oxide (Pd_5O_4) and three dimensional (3D) oxide (PdO) is an active area of research. Current work in our laboratory has provided insight on a previously unreported precursor state that leads to bulk oxidation. The precursor state appears to be oxygen chemisorbed on the 2D surface oxide, which is present up to coverages as high as 2 ML [22,27]. Depopulation of the precursor state begins at 1.5 ML and leads to the onset of particles that resemble the 3D bulk oxide [22]. Above this coverage range the surface is predominantly covered by 3D oxide [12].

Establishing an oxidized Pd surface in UHV conditions provides the opportunity to further probe different characteristics and interactions of the surface. For instance, real-world applications of Pd catalysis occur in environments with higher partial pressure of O_2 than those accessible in UHV. At these conditions, O_2 could adsorb molecularly on the oxidized surface and play an important role in subsequent surface chemical reactions. Further characterization of the oxidized surface can provide additional insight into these effects. The experiments discussed in this work evaluated the chemisorption of molecular oxygen and the oxidized surface. Key results from this study are that O_2 molecules bind more strongly on the oxide surface than on the metallic surface, that O_2 dissociation is negligible on the oxidized surface, and that O_2 chemisorbed on the oxide is reactive toward CO.

Experiment Equipment

The following provides details of the equipment and procedures used in this study, with further information provided in previous studies [18,21,28]. The UHV chamber is a three-level chamber that routinely reaches a base pressure below 2×10^{-10} Torr. Evacuation of the main chamber is provided by a combination of a 400 l/s ion pump, a 210 l/s turbo molecular pump, and a titanium sublimation pump contained within a liquid-nitrogen-cooled cryoshroud. The chamber is equipped with instrumentation for X-ray photoelectron spectroscopy (XPS), Auger electron spectroscopy (AES), electron energy loss spectroscopy (EELS), ion scattering spectroscopy (ISS), and low-energy electron diffraction (LEED). The chamber also contains a quadrupole mass spectrometer (QMS) used to monitor the concentrations of gases.

The main chamber has an additional two-stage differentially pumped chamber that contains an RF plasma source (Oxford Scientific Instruments). The plasma source is used to partially dissociate O_2 (BOC gases 99.999%) into highly reactive O atoms used in the oxidation of Pd(111). The dissociation capability of the plasma source has been estimated to be ≈ 20% [29]. The first pumping stage contains oppositely-charged ion deflection plates and is evacuated with a 1200 l/s diffusion pump. A 3 mm conical skimmer connects the first and second pumping stages, directing the beam into a quartz tube 60 mm in length with an inner diameter of 6 mm. The second pumping stage is evacuated using a 70 l/s turbo molecular pump. A mechanical shutter attached at the end of the first pumping stage controls the exposure of the surface to the atomic oxygen beam.

The Pd (111) crystal used in this study is a circular disk 8 mm × 1 mm purchased from Mateck GmbH. The crystal is polished on one side and has a surface roughness of less than 3 μm. The crystal is attached to a copper sample holder in thermal contact with a liquid nitrogen reservoir by spot-welding two tungsten wires to the backside of the crystal. A K-type

thermocouple spot-welded to the backside of the crystal is used to measure sample temperature. Resistive heating, controlled by a PID controller connected to a DC power supply, provides a linear temperature ramp from 85 K to 925 K, utilized in TPD. The sample holder is attached to a XYZ manipulator that allows for accurate positioning of the sample. Initial sample cleaning entails sputtering with Ar^+ ions at 600 eV and a sample temperature of 900 K and then annealing to 1100 K. Routine cleaning consisted of exposing the sample at 856 K to the atomic oxygen beam for 30 minutes, followed by annealing to 925 K. The sample is positioned approximately 50 mm from the end of the quartz tube within the UHV chamber at a 45° rotation to provide uniform exposure across the crystal surface. This position is monitored frequently to avoid non-uniform oxidation of the surface. The sample was considered clean when CO was no longer detected during an annealing cycle.

The focus of this study was molecular oxygen adsorption on an oxidized Pd(111) surface. The experiments conducted were oxygen adsorption on a 3 ML oxide-covered surface, oxygen adsorption on a variety of atomic oxygen coverages, mixed isotope adsorption, and oxygen co-adsorption with CO. These experiments required molecular oxygen and CO exposures as well as exposure to atomic oxygen. Atomic oxygen exposures were conducted at 500 K for a specified duration to produce a desired coverage, for example a 10 minute exposure routinely produced a 3 ML coverage. Molecular gases, exposed at 85 K had a typical $^{18}O_2$ exposure and $^{16}O_2$ exposure of less than 0.10 L and 61 ML respectively. TPD and TPRS measurements were obtained by placing the sample within 10 mm of the QMS ionizer and increasing the sample temperature at a linear rate of 1 K s^{-1}.

Data processing for TPD experiments entailed a straight line base line subtraction and 5 point adjacent averaging smoothing. Coverage calibration spectra were obtained by saturating

the clean surface at room temperature. The first calibration spectrum involved a triple cycle of saturation exposures using both $^{16}O_2$ and $^{18}O_2$ gas. The areas under the curve of these spectra were equated to a 0.25 ML coverage [12], from which area-coverage factors could be extracted for $^{16}O_2$, $^{16}O^{18}O$ and $^{18}O_2$. The other calibration coverage involved only using $^{16}O_2$ gas to saturate the surface at room temperature and this calibration factor was used in experiment that only implemented $^{16}O_2$.

CHAPTER 2
MOLECULAR CHEMISORPTION OF O_2 ON OXIDIZED PD(111)

Results and Discussion

Oxygen Adsorption on 3 ML Oxide-covered Surface

Shown in Figure 2-1 are O_2 TPD spectra obtained from clean and oxide-covered Pd(111) after exposing these surfaces to saturation doses of O_2 at 85 K. The oxide-covered surface had an initial atomic oxygen coverage of 3 ML. Considering differences in sample heating rates, our TPD spectrum from the O_2-exposed metal surface agrees well with those reported in prior studies [30,31]. For the metal surface, we observe two sharp desorption features, labeled as α_2 and α_1, centered at 120 K and 179 K, respectively, as well as a third broader feature (not shown) at about 750 K. A previous study established that the low temperature α_1 and α_2 features originate from molecularly chemisorbed O_2 on Pd(111), while the desorption feature near 750 K results from the recombinative desorption of chemisorbed oxygen atoms [31]. At 85 K, only molecularly chemisorbed O_2 exists on Pd(111), but a fraction of these species dissociate as the sample is heated during the TPD experiment, giving rise to the recombinative desorption feature near 750 K. From our data, we estimate a total oxygen coverage of 0.66 ML (O/Pd) at O_2 saturation of the metal surface at 85 K, with 0.42 ML evolving below 400 K. These values agree well with prior work by Guo *et al*. [30]. Notice also that we obtain a coverage of 0.24 ML of oxygen atoms produced by O_2 dissociation, in excellent agreement with the known O-atom saturation coverage of 0.25 ML on Pd(111) obtained with O_2 as the oxidant [12].

After the O_2 exposure at 85 K, the O_2 TPD spectrum obtained from the oxide-covered surface exhibits two prominent features (β_2 and β_1) with maxima at 118 K and 227 K, respectively, and shoulders, labeled as γ_1 and γ_2, centered at about 275K and 315 K, respectively. As discussed in more detail below, experiments using $^{18}O_2$ show that these features originate

from molecularly chemisorbed O_2, and that a negligible amount of the adsorbed O_2 molecules dissociates on the Pd oxide during heating. The O_2 TPD spectrum below 400 K is qualitatively similar to that obtained from the metal surface in that two main features are observed in each case. The β_2 feature is less intense than the analogous α_2 feature obtained from the metal surface, but both features appear at about 120 K in the TPD spectra and each is rather narrow. In contrast, the β_1 feature is much broader than the α_1 peak, and reaches a maximum at a temperature nearly 50 K higher than the α_1 state. This latter observation is intriguing since it implies that O_2 molecules chemisorbed in the β_1 state on PdO are more strongly bound than O_2 chemisorbed on metallic Pd(111). Finally, the data shown in Figure 2-1 yields an oxygen coverage of 0.26 ML (O/Pd) for O_2 that desorbs below 400 K from the oxide-covered surface. This value is lower than that for the metal surface, but it is a relatively large coverage in an absolute sense. As such, the strong O_2 binding in the β_1 state is difficult to rationalize in terms of O_2 adsorption on oxide defect sites such as oxygen vacancies.

Prior work using high resolution electron energy loss spectroscopy (HREELS) reveal distinct differences in the O_2 binding states on Pd(111) [32]. Specifically, O_2 chemisorbed in the α_1 and α_2 states exhibit O-O stretching frequencies of 650 cm^{-1} and 800 cm^{-1}, respectively [32]. The lower O-O stretching frequency of O_2 in the α_1 state suggests that the O-O bond is weaker for the O_2 molecules that are more strongly bound to the surface. Imbihl *et al.*[32] proposed that binding in the α_1 and α_2 states involves each O-atom of an O_2 molecule bonding to a different Pd atom versus the same Pd atom, respectively. Since the O-O stretching frequencies fall within the range expected for peroxo linkages, these authors referred to the binding configurations in the α_1 and α_2 states as “peroxo-II” and “peroxo-I”, respectively. A superoxo state of O_2 on Pd(111) has also been identified using HREELS [32] and is found to desorb at temperatures below the α_2

peak maximum [30]. However, we do not observe evidence for this state in TPD, which suggests possibly that O_2 molecules do not populate the superoxo state under the conditions we examined or that such species convert to the more strongly bound states before they can desorb during TPD.

The data obtained in the present study does not provide information for determining the O_2 binding configurations on the oxidized Pd surface. However, considering the qualitative similarities between the O_2 TPD spectra obtained from the metal and oxidized surfaces, it is conceivable that the β_1 and β_2 states are analogous to the peroxo-II and peroxo-I configurations identified for O_2 on Pd(111). If this is correct, the TPD data suggests that the peroxo-I species has a similar binding strength on the metal and oxide surfaces, while the peroxo-II species is more strongly bound on the oxide. This would be an interesting difference between O_2 chemisorbed on the metal versus oxide surfaces if O_2 does actually bind on the oxide in the peroxo configurations. Spectroscopic work is clearly needed to further characterize the bonding of O_2 on the oxidized surface. Interestingly, O_2 chemisorbed on the oxide does not measurably dissociate during heating even though the strong O_2-surface bond suggests a weakened O-O bond in the β_1 state. Most likely, O_2 dissociation is highly activated on the oxide. Finally, the small features (γ_1 and γ_2) in the O_2 TPD spectra may originate from a small concentration of O_2 molecules that are strongly bound to defects on the oxide surface.

Figure 2-2 shows $^{18}O_2$ TPD spectra obtained after exposing oxidized Pd(111) held at 85 K to various doses of $^{18}O_2$. The resulting $^{18}O_2$ coverages are stated in the figure. Prior to the $^{18}O_2$ exposures, we generated ^{16}O coverages of 3 ± 0.2 ML by exposing the Pd(111) sample to an ^{16}O atom beam with the surface held at 500 K. As seen in Figure 2-2, $^{18}O_2$ initially desorbs in a broad feature centered at 275 K. This desorption feature appears to consist of about three components

(β_1, γ_1, γ_2) centered at 250, 275 and 325 K, respectively, in the TPD spectrum obtained from 0.03 ML $^{18}O_2$. The β_1 feature, initially centered at 250 K, intensifies considerably and shifts toward lower temperature as the $^{18}O_2$ coverage increases, its maximum appearing at 233 K at a coverage of 0.16 ML. The γ_1 and γ_2 desorption features also intensify with coverage, but to a lesser extent than the β_1 feature. In the spectrum obtained from 0.16 ML $^{18}O_2$, the γ_2 peak is evident as a distinct shoulder at 325 K while superposition between the γ_1 and β_1 features appears to produce a single broad feature that is skewed toward high temperatures. Interestingly, the shift of the β_1 maximum from 250 to 233 K suggests that O_2 binding to the surface weakens with O_2 coverage. For first order desorption, the TPD peak temperature is independent of the coverage if the activation energy is constant.

As the coverage increases beyond 0.16 ML, a new desorption peak, labeled as β_2, appears at 120 K. Unlike the β_1 feature, the β_2 peak temperature does not shift appreciably with increasing coverage, suggesting that interactions among chemisorbed O_2 molecules have a negligible influence on desorption of the β_2 state. Both the β_1 and β_2 peaks intensify concurrently with increasing coverage until the $^{18}O_2$ layer saturates at 0.33 ML. Notice that this coverage is higher than that shown in Figure 2-1, indicating that the oxidized surface was not saturated in those experiments. The development of the high and low temperature desorption features is similar to that observed previously on clean Pd(111) [30,31]. On the metal surface, the α_1 state initially populates with increasing coverage, and then the α_1 and α_2 states populate simultaneously beyond a critical coverage. While this may suggest similarities in the O_2 binding states on the metal and oxidized Pd surfaces, the high temperature TPD feature obtained from the oxidized surface is clearly composed of three, possibly more, distinct features. This suggests

greater variability in the bonding environments or configurations for O_2 on the oxidized surface compared with the metal.

Mixed Isotope

To determine whether the low temperature O_2 desorption features arise from molecularly or atomically adsorbed species, we conducted TPD experiments using co-adsorbed $^{16}O_2$ and $^{18}O_2$. In these experiments, we first dosed $^{18}O_2$ onto the oxidized surface at 85 K to generate an $^{18}O_2$ coverage slightly below 0.16 ML. We then exposed the surface to a relatively large $^{16}O_2$ dose and performed TPD while monitoring masses 32, 34, and 36 amu. Representative TPD spectra are shown in Figure 2-3. The evolution of $^{16}O^{18}O$ is immeasurable below 400 K, confirming that the low temperature desorption features indeed arise from molecularly adsorbed O_2. The figure also shows the desorption signals above 500 K. Decomposition of the oxide produces the sharp $^{16}O_2$ feature centered at 760 K as detailed in other work from our group [22]. The small amount of $^{16}O^{18}O$ desorbing as the 3 ML oxide decomposes corresponds to approximately 0.005 ML of ^{18}O. This is consistent with the natural abundance of $^{18}O_2$, and hence indicates that O_2 molecules chemisorbed on oxidized Pd(111) dissociate to a negligible extent during heating. This is not surprising considering that Pd(111) cannot be oxidized with O_2 at partial pressures typical of dosing in UHV.

The TPD data also reveals that O_2 molecules interchange among the various adsorbed states at temperatures as low as 120 K. Specifically, from integration of the TPD data, we estimate that the initial exposures produced $^{18}O_2$ and $^{16}O_2$ coverages of 0.06 ML and 0.14 ML, respectively. Based on the data shown in Figure 2-2, the initial 0.06 ML of $^{18}O_2$ molecules populate only the β_1, γ_1 and γ_2 states, yet a fraction of the $^{18}O_2$ from the mixed layer desorbs in the β_2 peak (Figure 2-3). Thus, the addition of $^{16}O_2$ to the initial $^{18}O_2$ layer causes $^{18}O_2$ molecules

to populate the β_2 state. Notice also that the intensity of the β_1 feature relative to the γ features is higher in the $^{18}O_2$ spectrum of Figure 2-3 than that seen in the TPD spectrum obtained from a layer containing only 0.06 ML of O_2 (Figure 2-2). This suggests that a fraction of the $^{16}O_2$ molecules also displace $^{18}O_2$ molecules from the γ states. The interchange of O_2 among adsorbed states appears to be relatively facile since some interchange must occur below the β_2 desorption temperature of 120 K. However, differences in the β_1 to β_2 peak ratios in the $^{16}O_2$ and $^{18}O_2$ TPD spectra demonstrate that the interchange is not rapid enough to cause complete isotopic mixing. Interestingly, similar isotopic mixing behavior has been reported for O_2 on clean Pd(111) [30,31].

Oxygen Adsorption on Varied Oxide Coverages

To examine how the initial atomic oxygen phases on Pd(111) influence molecular O_2 chemisorption, we conducted a series of O_2 TPD experiments on surfaces with varying amounts of atomic oxygen. For these experiments, we first generated an atomic oxygen coverage on Pd(111) at 500 K using an ^{16}O atom beam, and then exposed the ^{16}O-covered surface held at 85 K to an $^{16}O_2$ exposure of 61 ML. We found that a 61 ML exposure was more than enough to saturate the 3 ML oxide on Pd(111) with chemisorbed O_2. The use of $^{16}O_2$, rather than $^{18}O_2$, for populating the molecular chemisorbed states was motivated largely by experimental convenience. In the experiments with $^{18}O_2$, it was necessary to stop the $^{16}O_2$ flow to the plasma source to avoid uptake of $^{16}O_2$ prior to the $^{18}O_2$ dose. By using $^{16}O_2$ as the molecular adsorbent, the residual $^{16}O_2$ uptake prior to the $^{16}O_2$ dose does not affect the TPD measurements and enabled us to stabilize a plasma at the start of the day, and maintain it for the duration of the experiments.

Figure 2-4 shows the saturation O_2 coverage obtained at 85 K as a function of the initial O atom coverage. Briefly, the evolution of atomic oxygen states on Pd(111) is known to initially involve O atoms arranging into a p(2×2) structure [12]. Increasing the O atom coverage beyond 0.25 ML then causes a so-called two-dimensional (2D) surface oxide to develop, which saturates at approximately 0.7 ML[23,25]. Prior studies show that the 2D oxide consists of a single layer of Pd and O atoms arranged on top of the Pd(111) surface [23,25]. The 2D oxide has a Pd_5O_4 stoichiometry, is incommensurate with the underlying (111) lattice, and its structure does not match any lattice plane of crystalline PdO [25]. Recently, our group has found evidence that O atoms adsorb on top of the 2D oxide as the oxygen coverage increases beyond 0.7 ML, and that these adsorbed O atoms react with the 2D oxide to produce three-dimensional (3D) oxide particles that resemble bulk PdO [22]. The 3D oxide particles grow on Pd(111) and coexist with O-atom covered 2D oxide domains as the coverage increases above 0.7 ML. Once the oxygen coverage reaches about 3 ML, the surface is predominantly covered by the 3D oxide, with 2D oxide covering, at most, a very small area of the surface [12]. Oxidation at 500 K effectively ceases at 3.4 ML for the O atom beam flux (~0.02 ML/s) employed in our experiments. However, we are able to generate higher oxygen atom coverages by oxidizing at surface temperatures above 500 K.

Figure 2-4 shows that the O_2 coverage obtained at 85 K depends sensitively on the initial atomic oxygen coverage. Initially increasing the coverage of chemisorbed O atoms to about 0.25 ML causes the O_2 coverage to drop precipitously from 0.66 ML to about 0.03 ML. The O_2 coverage remains low as the initial O atom coverage increases to about 1 ML, corresponding to growth of the 2D oxide and initial adsorption of O atoms on the 2D oxide. The O_2 coverage increases nearly linearly with initial O-atom coverage as 3D oxide particles grow on the surface

from 1 to 2.7 ML. The O_2 coverage then appears to rise more slowly in the O-atom coverage range from 2.7 to 3.4 ML, reaching a maximum of about 0.29 ML on the 3.4 ML oxide. Further increasing the atomic oxygen coverage apparently causes the saturation O_2 coverage to decrease again. Specifically, we find that the saturation O_2 coverage on surfaces with 8 and 19 ML of atomic oxygen is 0.20 ML, nearly 35% less than that obtained on the 3 ML oxide. We note, however, that the 8 and 19 ML oxides were prepared at surface temperatures of 650 and 700 K, respectively, so it is unclear if the decrease in O_2 uptake is associated with the preparation temperature, the initial O-atom coverage or both. For example, oxides prepared at higher surface temperature may be smoother and thereby provide less surface area for O_2 uptake.

Focusing on the data obtained below 3.5 ML, it is clear that the 2D and 3D oxides have distinct affinities toward binding O_2 molecules. This result indicates that the 2D and 3D oxides offer chemically distinct binding sites, and suggests that these oxides are likely to exhibit distinct catalytic properties as well. Interestingly, our group has recently characterized the 2D and 3D oxides using ion scattering spectroscopy (ISS), and find that the ratio of O/Pd ISS signals is about twice as high for the 3D oxide (at 3 ML) than the 2D oxide [22]. Assuming similarities in ion scattering cross sections and neutralization probabilities on the 2D and 3D oxides, this finding indicates that the concentration of exposed Pd atoms on the 3D oxide is roughly half that on the 2D oxide. Since the Pd concentration of the 2D oxide is 0.67 ML according to several prior studies [23,25], our ISS results predict a concentration of exposed Pd atoms of 0.33 ML for the 3D oxide at 3 ML total oxygen coverage. This value is remarkably close to the saturation O_2 coverage of ~0.3 ML (O/Pd) obtained on the 3 ML oxide, and hence implies that one surface Pd atom is available for each O-atom of the molecularly chemisorbed O_2 at saturation.

Desorption of O_2 below 400 K is shown in Figure 2-5 as a function of the initial O-atom coverage. For O-atom coverages between 0.25 and about 1 ML, only a small feature at about 120 K is evident in the TPD spectra. This feature is broader than the β_2 peak that populates at high coverage on the 3D oxide, though they appear at a similar temperature. Considering that such a small amount of O_2 desorbs in this regime, this O_2 may originate from defects in the chemisorbed O-atom layer or the 2D oxide. It is also possible that this O_2 evolves from the edges or backside of the crystal. As the amount of 3D oxide increases with increasing O-atom coverage from 1 to 3.4 ML, O_2 TPD features centered at 120 and 230 K simultaneously intensify. In fact, above an atomic oxygen coverage of 1.8 ML, the β_1 to β_2 intensity ratio remains approximately constant. Since 3D oxide particles grow in the presence of 2D oxide domains, the available surface area of the 3D oxide increases with total oxygen coverage. Thus, the TPD data suggests that O_2 molecules populate the same binding states at saturation of 3D oxide particles of varying size, and that the total O_2 coverage scales with the surface area of the 3D oxide particles present at a given O-atom coverage. The dependence of the O_2 saturation coverage on the initial O-atom coverage may provide insights for characterizing the surface morphological changes during growth of the 3D oxide.

CO Oxidation

The present study was motivated largely by the idea that molecularly chemisorbed O_2 could be a reactive species in catalytic processes that occur on oxidized Pd at commercially relevant pressures, including the catalytic oxidation of CO and CH_4. Our finding that O_2 molecules, in certain states, bind more strongly on PdO than Pd(111) supports the idea that molecularly chemisorbed O_2 can exist in appreciable concentrations on oxidized Pd at high pressure and temperature, and is therefore a viable reactant. To initially explore the reactivity of

chemisorbed O_2 on PdO, we examined the oxidation of CO on the oxidized Pd(111) surface using TPRS. For this study, we first examined the reaction of only CO with the ^{16}O oxidized surface, and then studied the reaction of CO co-adsorbed with $^{18}O_2$ on the ^{16}O oxidized surface. For each experiment, we first oxidized the Pd(111) sample at 500 K with an ^{16}O beam to reach an ^{16}O coverage of ~3 ML. We then exposed the oxidized surface held at 85 K to 0.01 L of $^{18}O_2$, followed by a 26 ML dose of $C^{16}O$. The same CO exposure was used in the experiments with and without co-adsorbed $^{18}O_2$, but resulted in different CO coverages as discussed below. Finally, after preparing the adsorbed layers, we heated the sample at a linear rate of 1 K s^{-1} while monitoring the partial pressures of $C^{16}O$, $^{16}O_2$, $^{18}O_2$, $C^{16}O_2$, $C^{18}O^{16}O$ and $C^{18}O_2$.

Figure 2-6 shows representative TPRS traces obtained in these experiments. The top panel shows the $C^{16}O_2$ desorption trace during TPRS with only adsorbed $C^{16}O$, while the bottom panel shows the TPRS traces of $C^{16}O_2$, $C^{18}O^{16}O$ and $^{18}O_2$ obtained during experiments with co-adsorbed $C^{16}O$ and $^{18}O_2$. Before discussing the TPRS data, it is important to clarify our quantitative analysis of this data and the rate scale used in Figure 2-6. As discussed above, we express the measured O_2 desorption signals in units of ML of O-atoms using the integrated signal obtained from Pd(111) with an assumed coverage of 0.25 ML of O-atoms, which we prepare using a well established procedure. To estimate the CO and CO_2 yields in ML of these species, we rescaled calibration factors determined in a recent study of CO oxidation on Pt(100) conducted in our laboratory [33]. Specifically, we assumed that the relationships among the O_2, CO and CO_2 scaling factors are the same in the present study as in our work with Pt(100), and then rescaled the CO and CO_2 factors using the value that we more recently measured for O_2. This procedure may introduce error in absolute CO and CO_2 yields, but such error should largely cancel when considering relative values. Using these scaling factors, we estimate that the 26 ML

CO exposures produce initial CO coverages of 0.24 ML and 0.44 ML, respectively, on the oxidized surface with and without co-adsorbed $^{18}O_2$. Thus, the adsorbed $^{18}O_2$ appears to suppress CO adsorption on the oxidized surface, possibly by blocking surface sites. Finally, to better compare the relative reactivity of the oxidized surface with and without $^{18}O_2$, we scaled the TPRS curves shown in Figure 2-6 by the initial CO coverages stated above.

Figure 2-6 shows that both $C^{16}O_2$ and $C^{18}O^{16}O$ evolve from the $^{18}O_2$ covered surface, indicating that both PdO and chemisorbed $^{18}O_2$ react with CO during TPRS. Recall that chemisorbed O_2 dissociates to a negligible extent on the oxidized surface (Figure 2-3) so the presence of co-adsorbed CO must facilitate cleavage of the O-O bond, resulting in the addition of ^{18}O to adsorbed $C^{16}O$. Importantly, we find that the evolution of $C^{18}O_2$ is negligible in these experiments, which implies that CO oxidation on oxidized Pd(111) does not involve C-O bond cleavage. The $C^{16}O_2$ desorption trace obtained without co-adsorbed $^{18}O_2$ exhibits three main features centered at about 117, 355, and 520 K (Figure 2-6A). In prior studies, we have found that desorption from the sample mounting wires as well as the initially high, transient heating rate are largely responsible for the sharp peak at 117 K [18,33]. Nevertheless, reaction between CO and the oxide likely contributes to the trailing edge of this signal. The feature at 355 K most likely originates from reactions between CO and O atoms of PdO, while the feature at 520 K is characteristic of reaction between CO and O atoms adsorbed on metallic sites produced as the oxide is reduced.

In addition to the initial sharp peak, the $C^{16}O_2$ spectrum obtained from the surface with adsorbed $^{18}O_2$ exhibits a broad feature centered at 320 K, and only low intensity above 500 K (Figure 2-6B). Since the initial CO coverage was lower in this experiment, the majority of the CO molecules likely reacted below 500 K thereby resulting in the diminution of the CO_2 signal

observed at 520 K in the experiment without co-adsorbed $^{18}O_2$. It is interesting that the intermediate $C^{16}O_2$ feature appears at 320 K in the presence of $^{18}O_2$, but is centered at 355 K and is more asymmetric when CO is adsorbed alone on the oxide. Neglecting differences in the CO coverages, this may indicate that the presence of chemisorbed $^{18}O_2$ influences the reaction of CO with the oxide. The $C^{18}O^{16}O$ spectrum also exhibits a broad feature at about 320 K as well as a less intense feature below 200 K. In this case, the intensity below 200 K, while small, is broad and overlaps the range of temperature over which chemisorbed $^{18}O_2$ desorbs, suggesting that this CO_2 originates mainly from reaction on the sample surface rather than the mounting wires. Finally, we note that the highest $C^{18}O^{16}O$ desorption rate occurs at 320 K, and mainly overlaps the trailing edge of the $^{18}O_2$ desorption feature.

Estimates of the product yields show that the oxidation of CO is relatively efficient on both surfaces studied. For example, on the surface without co-adsorbed O_2, we estimate that 57% of the adsorbed CO molecules react with the oxide to produce CO_2. In the presence of adsorbed $^{18}O_2$, approximately 40% of the CO molecules react with the oxide, while 15% react with ^{18}O to produce $C^{18}O^{16}O$. Interestingly, the total fraction of CO molecules that react is nearly equal on both surfaces for the conditions examined. The yields show that fewer CO molecules react with ^{18}O than ^{16}O of the oxide. However, to put this in perspective, it is necessary to estimate the amount of ^{16}O and ^{18}O atoms that are present at the surface. From the desorption yields of $C^{18}O^{16}O$ and $^{18}O_2$, we estimate that the initial ^{18}O coverage from $^{18}O_2$ molecules was 0.18 ML, whereas the reaction occurred on an oxide with 3 ML of ^{16}O atoms. However, only a fraction of the oxygen atoms are present at the surface of the oxide particles. Our recent ISS results show that the 3 ML oxide has about twice the surface concentration of atomic oxygen than the 2D oxide for which the O coverage is 0.58 ML according to recent studies [23,25]. Thus, based on

the ISS results, we estimate that the 3 ML oxide has an affective surface oxygen concentration near 1.2 ML. Most likely, this concentration exceeds 1 ML because the oxidized surface is rougher than the original Pd(111) surface. These estimates suggest that the surface concentration of ^{16}O atoms of the oxide was more than six times greater than the coverage of ^{18}O in the molecular oxygen chemisorbed on the oxide during the TPRS experiments. For comparison, the yield of $C^{16}O_2$ was approximately 2.7 times greater than the $C^{18}O^{16}O$ yield, indicating that the probability for CO to react with $^{18}O_2$ is higher than the CO reaction probability with oxygen atoms of PdO for the conditions studied.

These initial experiments clearly demonstrate that O_2 molecules chemisorbed on oxidized Pd(111) are reactive toward CO. However, more thorough studies are needed to elicit the detailed aspects of this reactive interaction. For example, it is conceivable that co-adsorbed CO and O_2 react directly on the oxide surface, possibly via a CO_3 intermediate, to produce CO_2 and an O atom. Another possibility, however, is that the reaction of CO with the oxide creates oxygen vacancies that are effective in activating the O_2 bond, even though O_2 dissociation on the oxide is otherwise negligible (vide supra). Overall, the findings of these preliminary experiments provide substantial motivation for conducting further investigations of the reactivity of O_2 molecules on oxidized transition metal surfaces, particularly considering the possibility that chemisorbed O_2 is an active catalytic species in commercial applications.

Summary

In this work, we utilized TPD and TPRS to investigate the chemisorption and reactivity of O_2 on oxidized Pd(111). The TPD data shows that O_2 binds more strongly in certain states to the oxidized surface than to the clean Pd surface, reaching a saturation coverage of 0.33 ML on Pd(111) covered with 3 ML of oxide. Experiments with co-adsorbed $^{16}O_2$ and $^{18}O_2$ reveal that O_2 molecules dissociate negligibly on the oxidized surface. The desorption of molecularly

chemisorbed O_2 gives rise to two main features centered at 118 K and 227 K as well as smaller features at 275 and 315 K. Interestingly, we find that O_2 molecules chemisorb only in small quantities on the 2D oxide on Pd(111), demonstrating that the 2D and 3D oxides are chemically distinct at least with respect to binding O_2. Finally, TPRS spectra provide clear evidence that both PdO and molecularly chemisorbed O_2 on the oxide are reactive toward CO, with the molecular species being slightly more reactive. This final, previously unreported observation warrants further investigation as it suggests that chemisorbed O_2 molecules could play a role in catalytic oxidation processes occurring at high pressure.

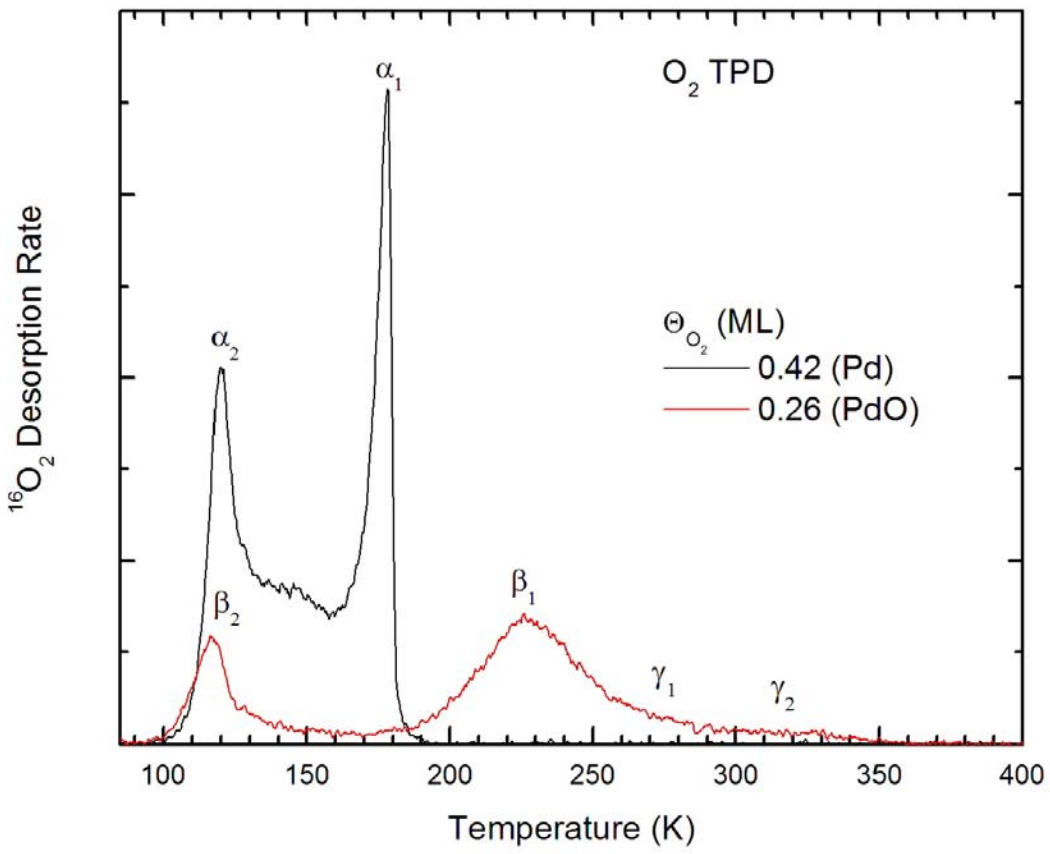

Figure 2-1. O_2 TPD spectra (heating rate = 1 K s^{-1}) obtained for a clean Pd(111) surface and a 3 ML PdO surface. The initial PdO surface was prepared by an exposure to atomic oxygen at 500 K which was then exposed to a saturation coverage of molecular oxygen. The total desorption quantity from all channels below 400K for the clean and PdO surface are 0.42 ML and 0.26 ML respectively.

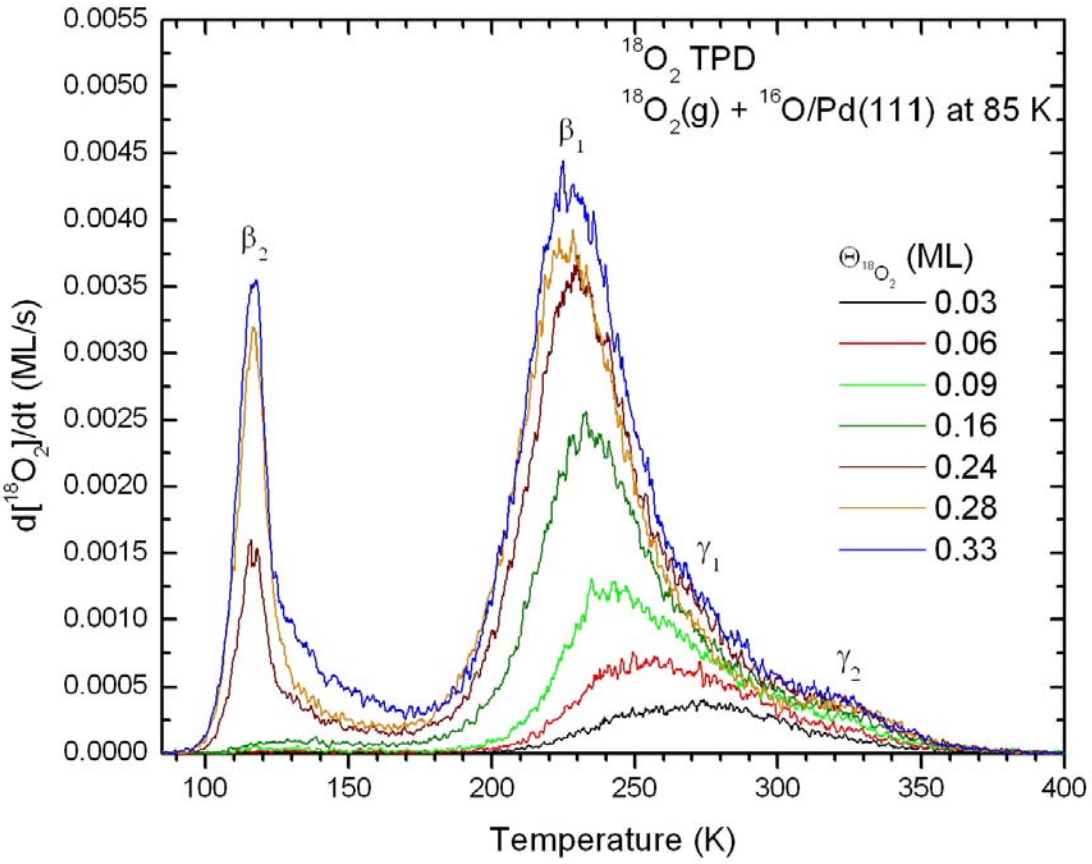

Figure 2-2. $^{18}O_2$ TPD spectra (heating rate 1 K s^{-1}) obtained by exposing Pd(111) to an atomic oxygen beam for 10 minutes at 500 K followed by various exposures of $^{18}O_2$ at 85 K. The initial molecular oxygen adsorption varied from 0.03 ML to 0.33 ML. The initial atomic oxygen coverage was calculated to be 3.0 ±0.20 ML.

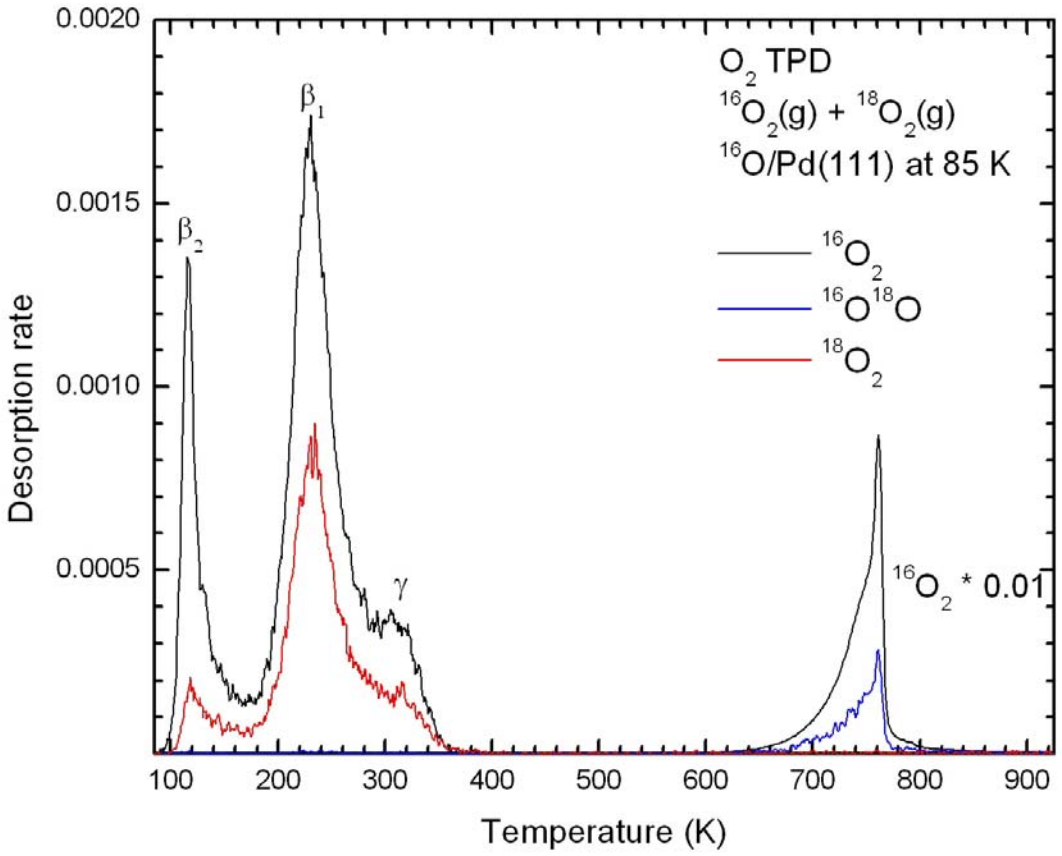

Figure 2-3. Mixed isotope O_2 TPD spectra (heating rate 1 K s^{-1}) obtained after exposing Pd(111) to an atomic oxygen beam at 500 K for 10 minutes. The sample was exposed to 0.015 L of $^{18}O_2$ followed by a saturation of $^{16}O_2$ at 85K. The calculated coverage for $^{16}O_2$ and $^{18}O_2$ below 500K was 0.14 ML and 0.06 respectively. A negligible amount of $^{16}O^{18}O$ was observed throughout the temperature range. Note the $^{16}O_2$ spectrum has been scaled by a multiplication factor of 0.01 after 400 K.

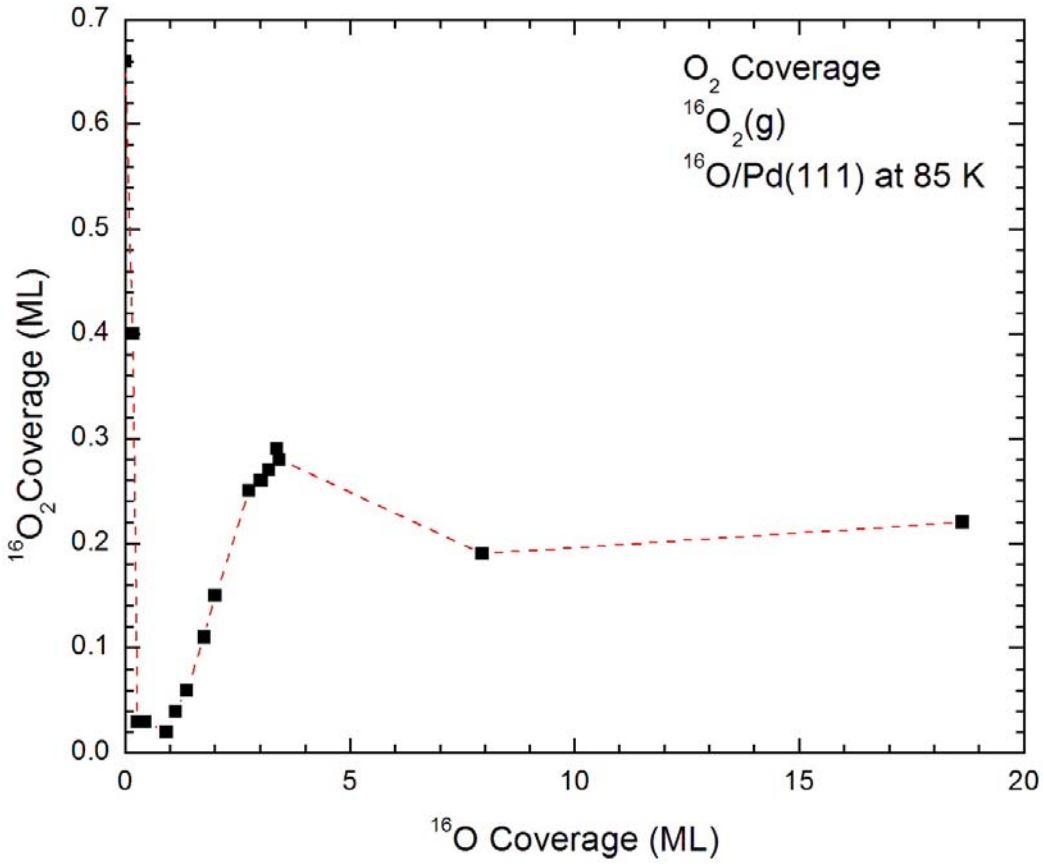

Figure 2-4. Oxygen uptake curve obtained by plotting the molecular oxygen coverage as a function of the atomic oxygen coverage on Pd(111). Coverages were calculated from TPD spectra obtained by exposing Pd(111) to various amounts of atomic oxygen at 500 K followed by a saturation $^{16}O_2$ exposure at 85 K.

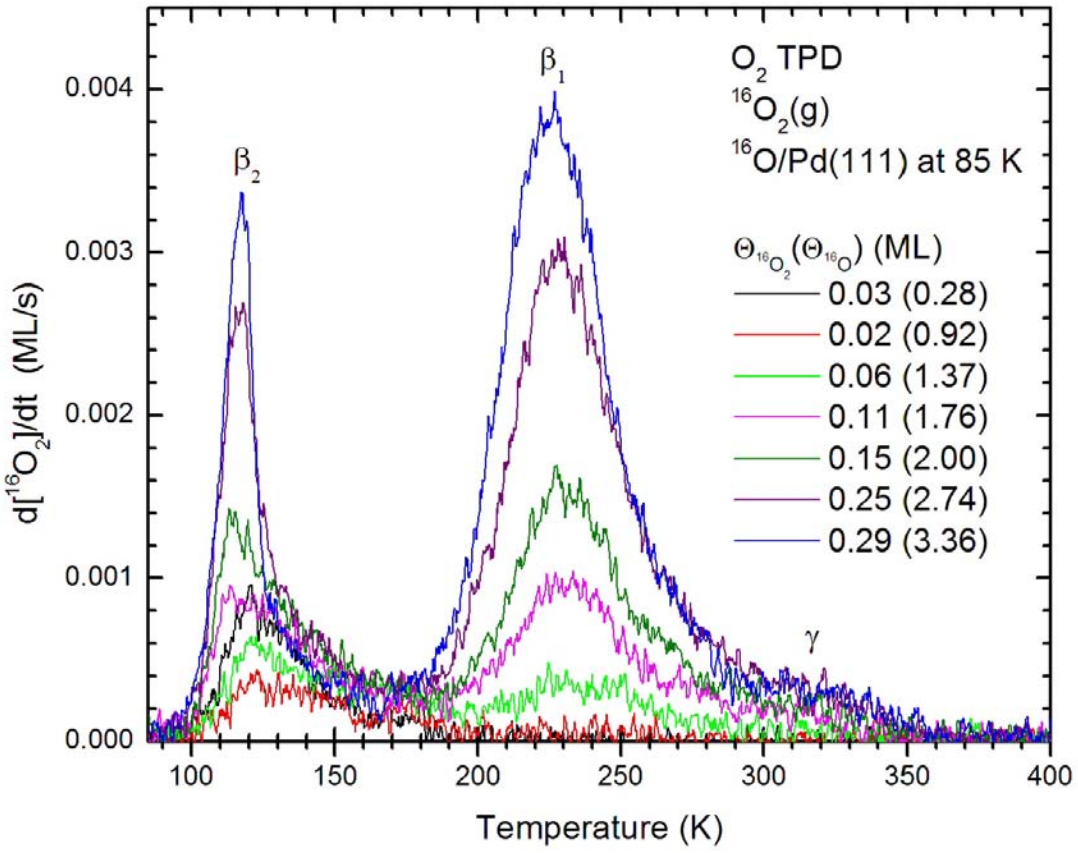

Figure 2-5. $^{16}O_2$ TPD spectra (heating rate 1 K s^{-1}) obtained by exposing Pd(111) to various amounts of atomic oxygen at 500 K followed by a saturation exposure of $^{16}O_2$ at 85 K. Initial atomic oxygen coverages range from 0.28 ML through 3.36 ML.

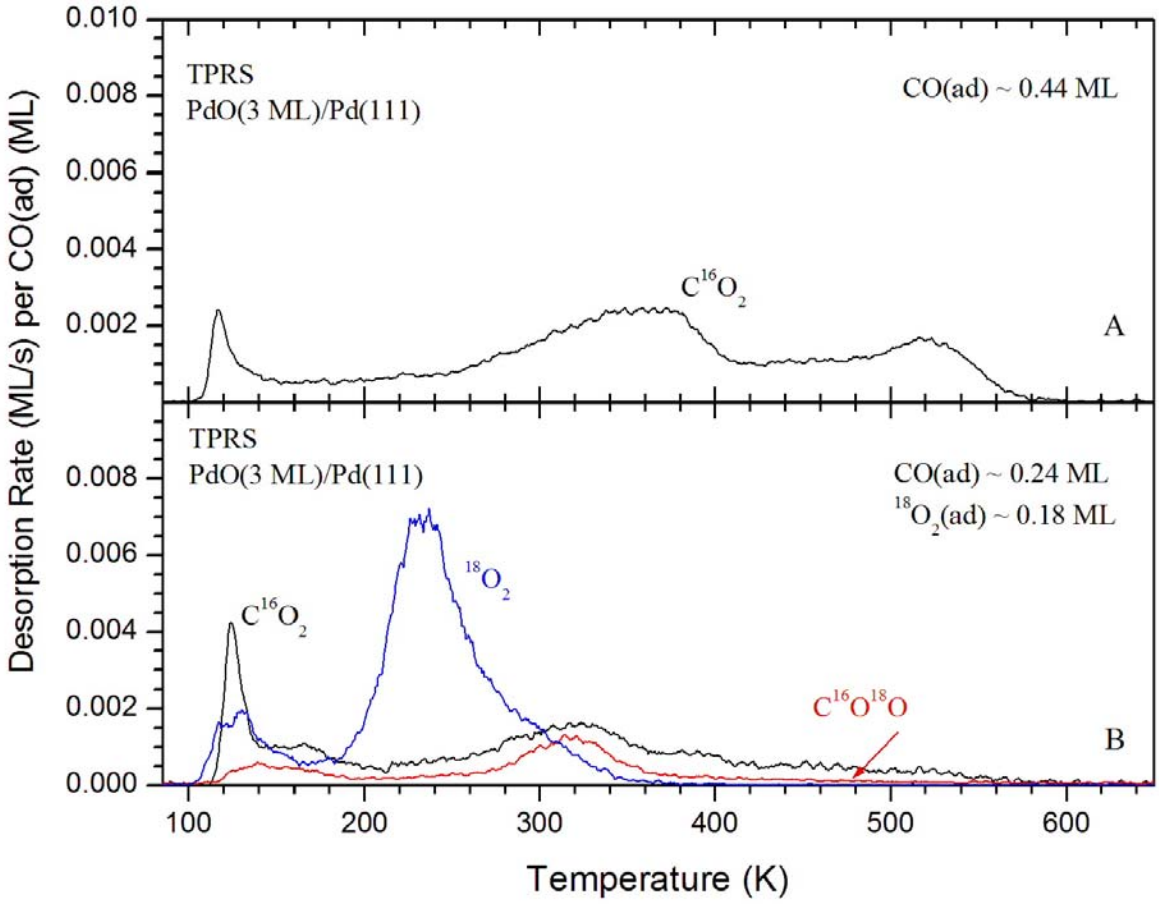

Figure 2-6. TPRS traces (heating rate = 1 K s^{-1}) obtained after initially exposing Pd(111) to an atomic oxygen beam for 10 minutes at 500 K. The oxidized surface was then exposed at 85 K to the following, A) a saturation exposure of CO B) a 0.01 L of $^{18}O_2$ followed by a saturation exposure of CO. The estimated initial atomic oxygen coverage was ≈3 ML for both TPRS traces.

LIST OF REFERENCES

[1] H. Gabasch, A. Knop-Gericke, R. Schlogl, M. Borasio, C. Weilach, G. Rupprechter, S. Penner, B. Jenewein, K. Hayek, B. Klotzer, Phys. Chem. Chem. Phys. 9 (2007) 533.

[2] K.W. Kolasinski, F. Cemic, A. Demeijere, E. Hasselbrink, Surf. Sci. 334 (1995) 19.

[3] I. Nakai, H. Kondoh, T. Shimada, A. Resta, J.N. Andersen, T. Ohta, J. Chem. Phys. 124 (2006) 224712.

[4] J.N. Carstens, S.C. Su, A.T. Bell, J. Catal. 176 (1998) 136.

[5] A.K. Datye, J. Bravo, T.R. Nelson, P. Atanasova, M. Lyubovsky, L. Pfefferle, Appl. Catal. A. 198 (2000) 179.

[6] R.J. Farrauto, J.K. Lampert, M.C. Hobson, E.M. Waterman, Appl. Catal. B. 6 (1995) 263.

[7] H. Gabasch, et al., J. Phys. Chem. C. 111 (2007) 7957.

[8] G.B. Hoflund, H.A.E. Hagelin, J.F. Weaver, G.N. Salaita, Appl. Surf. Sci. 205 (2003) 102.

[9] M. Lyubovsky, L. Pfefferle, Catal. Today 47 (1999) 29.

[10] J.G. McCarty, Catal. Today 26 (1995) 283.

[11] F.H. Ribeiro, M. Chow, R.A. Dallabetta, J. Catal. 146 (1994) 537.

[12] G. Zheng, E.I. Altman, Surf. Sci. 462 (2000) 151.

[13] H. Gabasch, et al., Surf. Sci. 600 (2006) 2980.

[14] R.F. Hicks, H.H. Qi, M.L. Young, R.G. Lee, J. Catal. 122 (1990) 280.

[15] S.H. Oh, P.J. Mitchell, R.M. Siewert, J. Catal. 132 (1991) 287.

[16] N. Saliba, Y.L. Tsai, C. Panja, B.E. Koel, Surf. Sci. 419 (1999) 79.

[17] J.Y. Han, D.Y. Zemlyanov, F.H. Ribeiro, Surf. Sci. 600 (2006) 2752.

[18] A.L. Gerrard, J.F. Weaver, J. Chem. Phys. 123 (2005) 224703.

[19] R.B. Shumbera, H.H. Kan, J.F. Weaver, Surf. Sci. 601 (2007) 235.

[20] J. Wang, Y. Yun, E.I. Altman, Surf. Sci. 601 (2007) 3497.

[21] J.F. Weaver, J.J. Chen, A.L. Gerrard, Surf. Sci. 592 (2005) 83.

[22] H.H. Kan, R.B. Shumbera, J.F. Weaver, in preparation.

[23] H. Gabasch, W. Unterberger, K. Hayek, B. Klotzer, G. Kresse, C. Klein, M. Schmid, P. Varga, Surf. Sci. 600 (2006) 205.

[24] J.Y. Han, D.Y. Zemlyanov, F.H. Ribeiro, Surf. Sci. 600 (2006) 2730.

[25] E. Lundgren, G. Kresse, C. Klein, M. Borg, J.N. Andersen, M. De Santis, Y. Gauthier, C. Konvicka, M. Schmid, P. Varga, Phys. Rev. Lett. 88 (2002) 246103.

[26] D. Zemlyanov, et al., Surf. Sci. 600 (2006) 983.

[27] R.B. Shumbera, H.H. Kan, J.F. Weaver, Surf. Sci. 601 (2007) 4809.

[28] A.L. Gerrard, J.J. Chen, J.F. Weaver, J. Phys. Chem. B. 109 (2005) 8017.

[29] H.H. Kan, R.B. Shumbera, J.F. Weaver, J. Chem. Phys. 126 (2007) 134704.

[30] X.C. Guo, A. Hoffman, J.T. Yates, J. Chem. Phys. 90 (1989) 5787.

[31] T. Matsushima, Surf. Sci. 157 (1985) 297.

[32] R. Imbihl, J.E. Demuth, Surf. Sci. 173 (1986) 395.

[33] R.B. Shumbera, H.H. Kan, J.F. Weaver, J. Phys. Chem. C. submitted.

BIOGRAPHICAL SKETCH

Jose A. Hinojosa Jr. was born on July 22, 1982, in Houston, Texas, to Jose A. Hinojosa and Adelaida Hinojosa. He graduated from South Houston High School in 2000 and continued his education at the University of Houston. In May 2005 he received his Bachelors of Science in chemical engineering. Jose and Beverly Brooks were married in July 2005 before continuing his education at the University of Florida. In December 2005 he began working for Dr. Jason F. Weaver, performing surface science research.